Accepted Manuscript

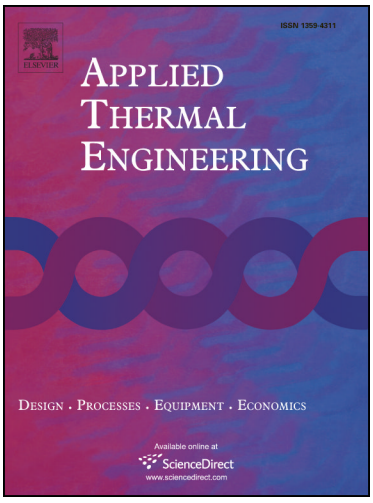

Determination of heat transfer coefficients in direct contact latent heat storage systems

Sven Kunkel, Tobias Teumer, Patrick Dörnhofer, Kerstin Schlachter, Yohana Weldeslasie, Martin Kühr, Matthias Rädle, Jens-Uwe Repke

PII: S1359-4311(18)33099-0
DOI: https://doi.org/10.1016/j.applthermaleng.2018.09.015
Reference: ATE 12624

To appear in: *Applied Thermal Engineering*

Received Date: 18 May 2018
Revised Date: 9 August 2018
Accepted Date: 3 September 2018

Please cite this article as: S. Kunkel, T. Teumer, P. Dörnhofer, K. Schlachter, Y. Weldeslasie, M. Kühr, M. Rädle, J-U. Repke, Determination of heat transfer coefficients in direct contact latent heat storage systems, *Applied Thermal Engineering* (2018), doi: https://doi.org/10.1016/j.applthermaleng.2018.09.015

This is a PDF file of an unedited manuscript that has been accepted for publication. As a service to our customers we are providing this early version of the manuscript. The manuscript will undergo copyediting, typesetting, and review of the resulting proof before it is published in its final form. Please note that during the production process errors may be discovered which could affect the content, and all legal disclaimers that apply to the journal pertain.

ACCEPTED MANUSCRIPT

Determination of heat transfer coefficients in direct contact latent heat storage systems

Authors

Sven Kunkel[1,*], Tobias Teumer[1], Patrick Dörnhofer[1], Kerstin Schlachter[1], Yohana Weldeslasie[1], Martin Kühr[1], Matthias Rädle[1], Jens-Uwe Repke[2]

[1]Sven Kunkel, Tobias Teumer, Patrick Dörnhofer, Kerstin Schlachter, Yohana Weldeslasie, Martin Kühr, Prof. Dr. rer. nat. Matthias Rädle, Hochschule Mannheim – University of Applied Sciences, Institute for Process Control and Innovative Energy Conversion, Paul-Wittsack-Straße 10, 68163 Mannheim, Germany

[2]Prof. Dr.-Ing. Jens-Uwe Repke, Technische Universität Berlin, Process Dynamics and Operations Group, Straße des 17. Juni 135, 10623 Berlin, Germany

*Corresponding author: Sven Kunkel, e-mail address: s.kunkel@hs-mannheim.de

Abstract

This study presents a novel concept for a direct contact latent heat storage, which can be used for storing thermal energy from industrial waste heat or renewable energy systems. A storage medium, phase change material (PCM), and mineral oil heat transfer fluid (HTF) are placed in direct contact. The PCM and the oil are not miscible. The direct contact leads to an improved heat transfer and faster loading and unloading periods with a high storage density. Only affordable salt hydrates or mixtures of salt hydrates and additives are used as the PCM. For the scaling of the system, the heat transfer coefficient of the complex system must be known. A cylindrical channel inside the PCM is created, and the heat transfer coefficients between the oil and solid or melting PCM is investigated. Subsequently, the transmission in a real channel is described and discussed.

Keywords: Direct contact heat storage, heat transfer coefficient, latent heat storage, near infrared, optical temperature measurement, phase change material

ACCEPTED MANUSCRIPT

ACCEPTED MANUSCRIPT

Nomenclature

A	Heat transfer area (m²)
$c_{p,HTO}$	Specific heat of the heat transfer fluid (HTF) (kJ/kg K)
d_c	Diameter of the PCM channel (mm)
$d_{c,crit}$	Critical diameter of the PCM channel (mm)
d_s	Diameter of the storage tank (mm)
Gz	Graetz number (-)
K_T	Factor of the temperature dependence of the material values
L	Characteristic length (mm)
$\dot{m}_{HTF}$	Mass flow HTF (kg/s)
Nu	Nußelt number (-)
Nu_0	Basic value of the Nußelt number (-)
$\mathrm{Pr}\ (\vartheta_{oil,in})$	Prandtl number at $\vartheta_{oil,in}$ (-)
$\mathrm{Pr}\ (\vartheta_{oil,out})$	Prandtl number at $\vartheta_{oil,out}$ (-)
Pr_m	Mean Prandtl number (-)
Pr_w	Prandtl number at ϑ_W (-)
$\dot{Q}$	Heat flow (W)
ΔQ_{latent}	Heat quantity, latent heat storage (kJ)
$\Delta Q_{sensible}$	Heat quantity, sensible storage (kJ)
r_c	Radius of the PCM channel (mm)
r_{PCM}	Distance from the middle of the channel to the temperature measurement point in the PCM (mm)
Re	Reynolds number (-)
v_{melt}	Melting velocity [mm/s]
α	Heat transfer coefficient (W/m²K)
α_{11}	Heat transfer coefficient at a height of 11 cm (W/m²K)
α_{16}	Heat transfer coefficient at a height of 16 cm (W/m²K)
α_{21}	Heat transfer coefficient at a height of 21 cm (W/m²K)
$\Delta\vartheta$	Temperature difference (K)
ϑ_m	Melting point temperature (°C)
$\vartheta_{F,8.i-1}$	Temperature of HTF at measurement point 8.i-1 (°C)
$\vartheta_{F,8.i}$	Temperature of HTF at measurement point 8.i (°C)

ACCEPTED MANUSCRIPT

ACCEPTED MANUSCRIPT

$\vartheta_{F,8.i+1}$	Temperature of HTF at measurement point 8.i+1 (°C)
$\vartheta_{PCM,8.i+1}$	Temperature of PCM at measurement point 8.i+1 (°C)
$\vartheta_{PCM,8.i}$	Temperature of PCM at measurement point 8.i (°C)
$\vartheta_{PCM,8.i-1}$	Temperature of PCM at measurement point 8.i-1 (°C)
ϑ_{W}	Temperature of the PCM wall (°C)
$\vartheta_{W,8.i}$	Temperature of the PCM wall at measurement point 8.i (°C)
λ_{HTF}	Thermal conductivity of HTF (W/m K)
λ_{PCM}	Thermal conductivity of PCM (W/m K)
t	Time [s]

Abbreviations

D/A	Digital/analog
HTF	Heat transfer fluid
$InGaAs$	Indium gallium arsenide
P	Pressure gauge
PC	Personal computer
PCM	Phase change material
T	Thermocouple

ACCEPTED MANUSCRIPT

ACCEPTED MANUSCRIPT

1 Introduction

Storage of thermal energy is an important issue for the upcoming energy transition in Germany, due to an increased use of renewable energy sources instead of fossil fuels. Furthermore, the use of industrial waste heat is desirable to reduce the number of primary energy sources and corresponding amount of greenhouse gases produced. Consequently, it is necessary to provide storage technology to synchronize the supply and demand of thermal energy. In general, there are three main types of thermal storage [1]:

- sensible heat storage
- latent heat storage
- thermochemical storage

Despite high storage densities of approximately 500 kWh/m³, thermochemical storage systems have the major disadvantage that the technology is complex and not mature [2]. Compared to sensible heat storage, latent heat storage systems provide the following advantages [3]:

- removal and supply of thermal energy at an approximately constant temperature
- high storage density that is ~50–100 times greater than that in sensible heat storage

Figure 1 shows, in principle, the difference between sensible and latent heat storage for the supply and removal of thermal energy. With sensible storage, energy supply results in a continuous nearly linear temperature increase. However, with latent heat storage, energy supply results in a temperature increase until the melting temperature of the PCM is reached. After that point, additional energy supply results in phase change without a further increase in temperature until the material is fully melted, after which the temperature again increases. It can be seen that a smaller temperature difference, $\Delta\vartheta$, between a loaded and unloaded latent heat storage results in a higher stored energy, ΔQ_{latent}, compared to the stored energy, $\Delta Q_{sensible}$, of a sensible heat storage. This is because latent heat storage makes use of the phase change enthalpy of the PCM.

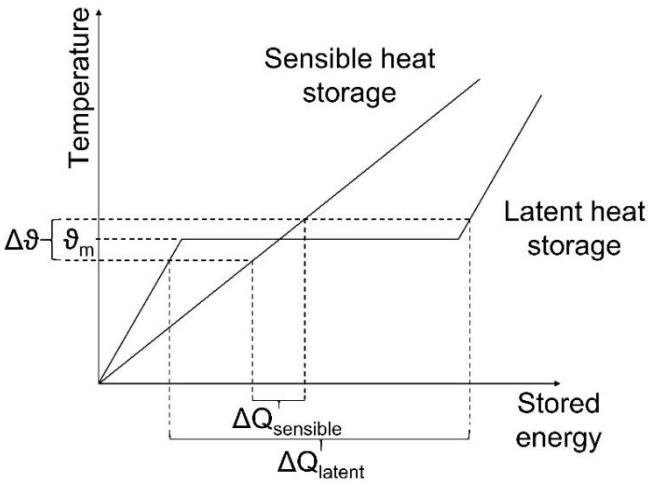

Figure 1: Difference between sensible heat storage and latent heat storage [4]

Fundamentally, there are two concepts for latent heat storage. In the first concept, the storage medium and the heat transfer fluid (HTF) are in indirect contact. The advantage of this system is the higher volume flow of the HTF, which leads to improved heat transfer

ACCEPTED MANUSCRIPT

between the PCM and the HTF. The disadvantage is that there is a wall between the PCM and the HTF, which leads to deteriorated heat transfer. In the second concept, the storage medium and the HTF are in direct contact. The absence of a wall between the storage medium and the HTF leads to improved heat transfer and faster loading and unloading periods with a high storage density.

Furthermore, direct contact storage has a simple structure with only an inlet and outlet for the oil. As there is no heat transfer pipe inside the storage tank, there is a larger space available for the PCM. This study is focused on direct contact latent heat storage. The first patented construction of a direct contact latent heat storage described in [5]. Figure 2 shows the basic structure of this first patented device. Different modifications and advantageous developments of the basic construction are also explained in the patent. A horizontal cylinder is proposed as a storage tank. The liquid HTF is circulated by a pump and is in direct contact with the storage medium, which can be a Glauber's salt solution. The HTF is introduced into the lower part of the storage tank through a pipe with openings, which serves as a distribution system for the HTF. In order to remove or supply thermal energy to the HTF, a heat exchanger is installed in a layer of the HTF (i.e., the heat exchanger medium).

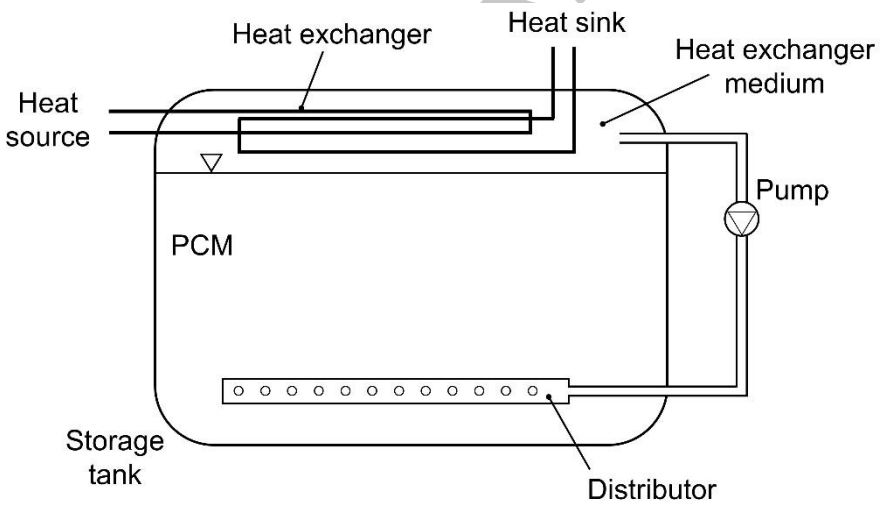

Figure 2: Basic construction of the first patented direct contact latent heat storage [5]

In [6], a storage tank with crystallization elements is described. Figure 3 shows the crystallization elements (no. 40) in the storage tank (FIG. 2) and in detail (FIG. 3).

ACCEPTED MANUSCRIPT

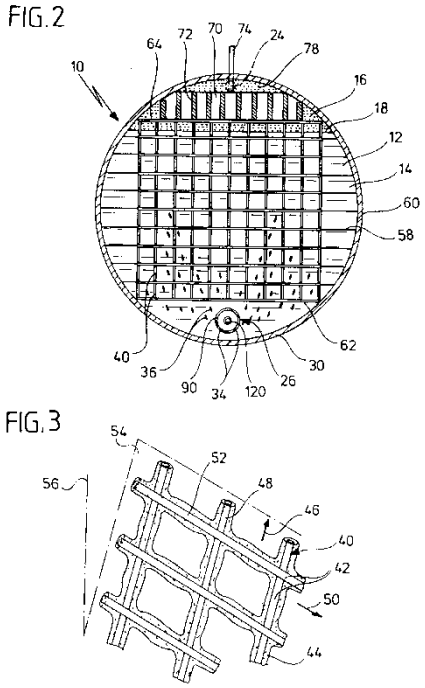

Figure 3: Sketch of the crystallization elements in the storage tank (FIG. 2) and in detail (FIG. 3) [6]

These crystallization elements are used to prevent a crystal slush from forming at the bottom of the storage tank. A horizontal cylinder is also employed as a storage tank. Using a salt hydrate in combination with an oil as the HTF is proposed. In this case, the HTF passes through a central tube in the lower part of the storage and branches into three feeds. However, introduction of the crystallization elements makes the system quite complex owing to their intricate structure. In addition, PCM volume is lost with introduction of the crystallization elements, resulting in a decrease in storage density. In [7], a concept for transporting thermal energy utilizing a direct contact latent heat storage is proposed. The storage medium is a sugar alcohol with a melting point of 118 °C, and the HTF is an oil. The aim of this system is location-independent use of industrial waste heat. The storage in the laboratory setup is also a horizontal cylinder with a diameter of 840 mm and a length of 150 mm. The supply of HTF is realized through two pipes with 3 or 6 oil outlet openings in the lower region of the storage. The HTF does not flow through the PCM evenly, which causes large areas of the PCM to melt late. This reduces storage performance and leads to a lower power during loading and unloading of the storage. The latent heat of the PCM is 473 kJ/L. A lab-scale direct contact latent heat storage system in which a sugar alcohol (melting point: 118 °C) is used as the storage medium and an oil is used as the HTF is described in [8-10]. Distribution of HTF in the storage is ensured by a branched piping system with downward-facing openings. In this device, the focus is the storing of thermal waste heat. The latent heat of the PCM is again 473 kJ/L. In [11], a direct contact latent heat storage used to store thermal energy at low temperatures is described. A paraffin with a melting point of 7 °C is used as the storage medium. The latent heat of the paraffin is 101 kJ/L. Water is used as the HTF. This concept differs significantly in its structural design owing to the lower density of the storage medium, and as a result the HTF is supplied into the storage from above.

In the literature, various concepts of direct contact latent heat storage have been described and characterized through measurements. However, there are no available measurements of the heat transfer coefficient between the PCM and the HTF. To improve the design and

ACCEPTED MANUSCRIPT

performance of a specially developed direct contact latent heat storage [12, 13], the heat transfer coefficient between solid or melting PCM and the HTF (an oil) is investigated. Initially, there is a solid PCM and a liquid oil phase. Melting provides an additional liquid PCM phase and affects the heat transfer.

To determine the heat transfer coefficient, a storage tank has been built which has only one oil supply at its bottom. To describe the heat transfer coefficient between the oil and PCM, an artificial cylindrical channel with a diameter of 6 mm is generated in the PCM. In this case, the heat transfer area is known. To determine the heat transfer coefficient between the PCM and oil, it is necessary to detect the temperature of the ascending oil phase within the channel. This study uses an optical measurement method that detects the radiation emitted by the oil in the near-infrared range (wavelength range: 1.6–2.2 µm) and converts it to a temperature. The detection of heat radiation in the near-infrared range has the advantage that it can be measured using a stiff glass fiber. By using a glass fiber, a precise temperature can be obtained without the measurement errors associated with the heat conducting properties of metallic sensors. Furthermore, the temperature within the PCM is measured with thermocouples to draw conclusions about the wall temperature of the channel.

Material and Methods

Material

In this study, a eutectic mixture of two salt hydrates (magnesium nitrate hexahydrate and magnesium chloride hexahydrate) is used as the PCM. A mineral oil (Fragoltherm Q-7) is used as the HTF, which was specially designed for the cooling and heating of process engineering plants. The PCM is not miscible with the oil. The essential substance characteristics of the eutectic mixture and the mineral oil are summarized in Table 1 [14, 15].

Table 1: Material properties of the PCM and oil

	PCM	Oil
Melting Point [°C]	59	-
Enthalpy [kJ/kg]	132	-
Heat capacity solid [kJ/kg·K]	2.5	-
Heat capacity liquid [kJ/kg·K]	3.0	2.221 (60 °C)
Heat conductivity solid [W/mK]	0.678 (38 °C)	-
Heat conductivity liquid [W/mK]	0.510 (65 °C)	0.124 (60 °C)
Density liquid [kg/m³]	1550	803 (60 °C)
Density solid [kg/m³]	1630	-

Experimental setup and measurement method

Figure 4 shows a schematic of the experimental setup. The setup consists of an oil receiver tank (A), an electrical gear pump (B), two heat exchangers (C and D) and the storage tank (E) containing the PCM. The storage tank is 350 mm high and has an inside diameter of 40 mm. The bottom of the storage tank has a hole with a diameter of 6 mm through which the oil enters the storage tank.

ACCEPTED MANUSCRIPT

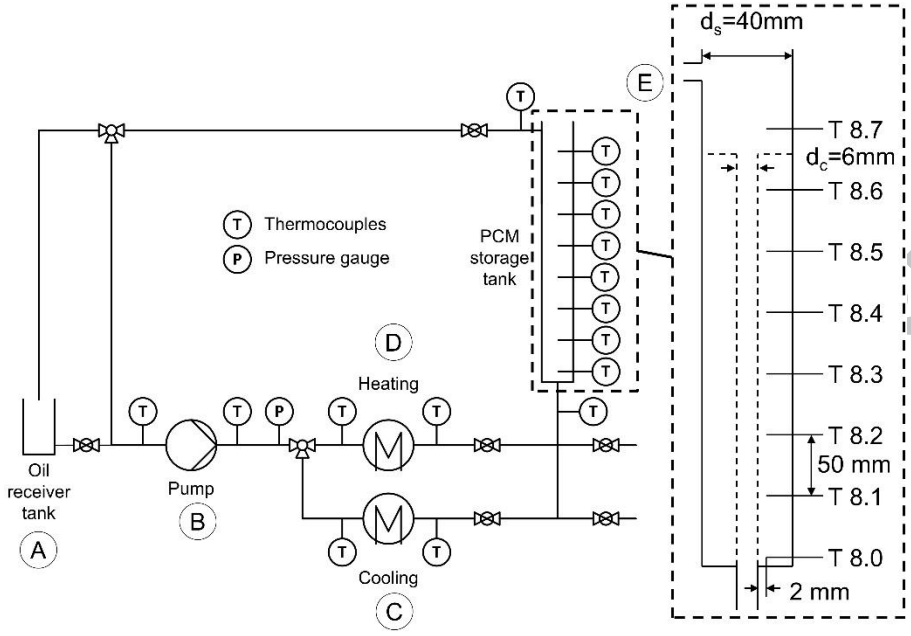

Figure 4: Schematic of the experimental setup

Seven thermocouples (type K) are installed in the storage tank to record the PCM temperature. Figure 4 also shows the configuration of the thermocouples in the storage tank. Temperature measurements acquired at locations 8.0 and 8.6 were not used in the determination of the heat transfer coefficient because they were susceptible to surrounding external influences. The thermocouple (type K) at location 8.7 is used for recording the oil temperature above the PCM. To obtain the mass flow of the oil, the known relationship between pump speed and mass flow was used. A calibration of the pump has been realized under test conditions to determine the relationship between pump specific flow rate and mass flow. To determine the heat transfer coefficient, an artificial channel with an inner diameter of 6 mm was made within the PCM. To build the channel, it is necessary that the PCM is liquid and oil is flowing into the storage tank. A steel tube with an outer diameter of 6 mm is then placed in the hole in the bottom of the storage tank so that the oil flows through the tube. By subsequently introducing cold oil, it is possible to remove thermal energy from the PCM until the PCM crystallizes around the tube. Once the entire PCM is solid, it is possible to remove the tube. Now there is a channel made of PCM. It is also necessary to measure the oil temperature flowing into the channel for the respective temperature measurements at each height within the PCM. Each measurement of the oil temperature takes about 2 s. At each height, the oil temperature is measured five times. The radiation emitted by the oil is detected in the wavelength range from 1.6–2.2 µm to determine the oil temperature. The oil layer in the channel leads to a transmission that approached zero in the considered wavelength range, which is the reason that only the oil temperature at the end of the glass fiber is measured.
From [16], it follows that a good absorber also represents a good emitter, and thus the relationship between the total emitted radiation and the temperature can be obtained.

The infrared sensor (an extended indium gallium arsenide (InGaAs) photodiode) and its components are illustrated in Figure 5. The measured data were collected by software developed in-house (National Instruments, LabView).

ACCEPTED MANUSCRIPT

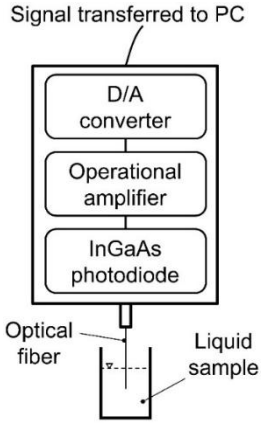

Figure 5: Schematic illustration of the infrared sensor and its components

Figure 6 shows the relationship between the infrared measurement signal and the oil temperature. The function represents the calibration, which allows each infrared measurement signal to be assigned a corresponding oil temperature. In this case, the glass fiber and a thermocouple are coupled and guided into the channel together.

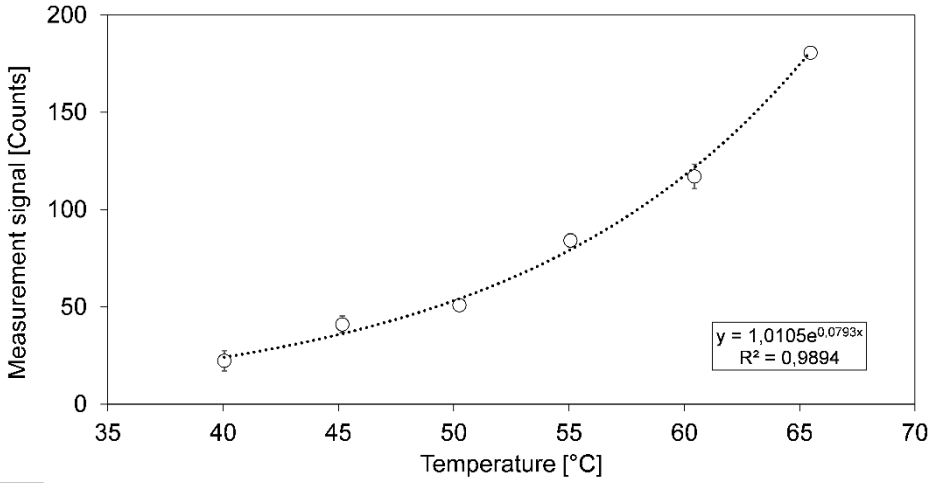

Figure 6: Infrared measurements as a function of the oil temperature

Four different measurements were carried out (measurements 1–4). During measurement 1, the heat transfer coefficient for solid PCM at an oil mass flow of 4.03×10^{-4} kg/s is investigated. Therefore, the inlet temperature of the oil is 56 °C and the initial temperature of the PCM is 20 °C. The heated oil is then introduced into the storage tank, and the temperature of the oil and the PCM are measured.

For measurements 2 and 3, the oil mass flows are 7.11×10^{-4} kg/s and 11.5×10^{-4} kg/s, respectively. All other conditions are the same as for measurement 1. From these measurements, the effect of the flow velocity on the heat transfer coefficient can be determined. The measurement results are shown in Figure 11.

In measurement 4, the inlet temperature of the oil is 75 °C and the oil mass flow is 6.50×10^{-4} kg/s. During this measurement, the PCM is melting. The initial temperature of the PCM is 20 °C. The heated oil is then introduced into the storage tank, and the temperature of the oil

ACCEPTED MANUSCRIPT

and the PCM are measured. This measurement investigates the effect of the liquid PCM on the heat transfer coefficient. The measurement results are shown in Figure 10. Table 2 summarizes the experimental conditions for each measurement.

Table 2: Experimental conditions

Measurement no.	Oil mass flow x 10^{-4} [kg/s]	Oil temperature [°C]	Re [-]
1	4.03	56	19
2	7.11	56	34
3	11.5	56	55
4	6.50	75	31

As Table 2 indicates, the measurements conditions produce a purely laminar flow within the channel.

Evaluation method

Figure 7 shows an explanation of the evaluation method, illustrating how the heat transfer coefficient can be calculated from the measured temperatures in the oil and the PCM. The left side of Figure 7 shows the storage tank with the PCM temperature measuring points. It can be seen that the heat transfer coefficient, α, can be determined over the channel height in three sections. The first heat transfer coefficient is at a measurement distance of x = 11 cm (α_{11}). Values for α_{16} (x = 16 cm) und α_{21} (x = 21 cm) are also obtained. The dashed box shows a detail view of the relevant measuring points for determining the heat transfer coefficients.

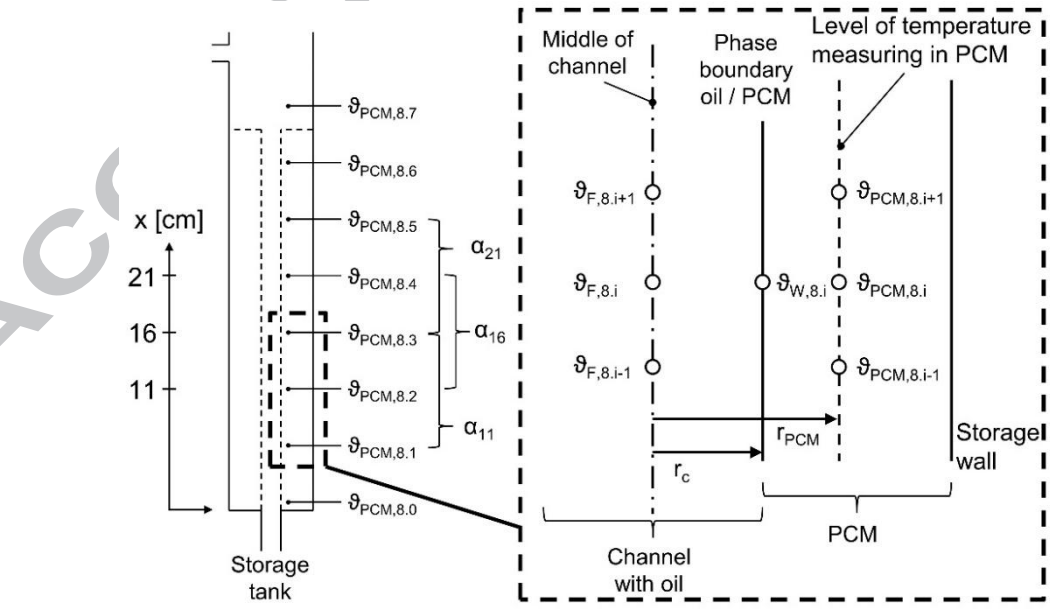

Figure 7: Representation of the channel and the relevant measuring points for measuring the heat transfer coefficient

ACCEPTED MANUSCRIPT

From the measured PCM temperature at point $\vartheta_{PCM,8.i}$, the known thermal conductivity of the PCM, λ_{PCM}, and the layer thickness of the PCM, the wall temperature in the PCM channel can be calculated as follows:

$$\dot{Q} = \frac{\lambda_{PCM} \cdot 2\pi L}{ln\frac{2 \cdot r_{PCM}}{2 \cdot r_c}} \cdot \left(\vartheta_{W,8.i} - \vartheta_{PCM,8.i}\right) \quad (1)$$

$$\vartheta_{W,8.i} = \frac{\dot{Q} \cdot ln\frac{2 \cdot r_{PCM}}{2 \cdot r_c}}{\lambda_{PCM} \cdot 2\pi L} + \vartheta_{PCM,8.i} \quad (2)$$

To determine the heat transfer coefficient, α, it is necessary to optically measure the oil temperature at point $\vartheta_{F,8.i}$. In these measurements $\vartheta_{F,8.i}$ is approximately the bulk mean temperature, because the glass fiber detected the oil temperature over a cross-sectional area. In addition, the glass fiber is not completely fixed in the middle of the channel. There is only a distance piece around the glass fiber, therefore the glass fiber can move within the channel increasing the overall accuracy, but not reach the PCM wall. According to equation (4), the heat transfer coefficient, α, can then be calculated. In this case the surface area, A, is known.

$$\dot{Q} = \alpha \cdot A \cdot \left(\vartheta_{F,8.i} - \vartheta_{W,8.i}\right) \quad (3)$$

$$\alpha = \frac{\dot{Q}}{A \cdot \left(\vartheta_{F,8.i} - \vartheta_{W,8.i}\right)} \quad (4)$$

By melting the PCM the surface area, A, is not constant. In this case the time is measured in which the defined PCM layer $r_{PCM} - r_c$ (see Figure 7) between the temperature measurement points $\vartheta_{PCM,8.i}$ and the channel inner wall has melted. The time t at which the PCM finished melting is used for calculation of the melting velocity in radial direction. The melting velocity v_{melt} is defined as follwos:

$$v_{melt} = \frac{r_{PCM} - r_c}{t} \quad (5)$$

With this velocity it is possible to get a function of the channel radius r=r(x,t) for each measuring point and time step and the heat transfer surface can be calculated.

To determine the transferred heat flow, the temperature of the oil is measured optically at locations $\vartheta_{F,8.i-1}$ and $\vartheta_{F,8.i+1}$, and the heat flow is calculated according to equation (6):

ACCEPTED MANUSCRIPT

$$\dot{Q} = \dot{m}_{HTF} \cdot c_{p,HTF} \cdot \Delta\vartheta \; wiht \; \Delta\vartheta = \vartheta_{F,8.i+1} - \vartheta_{F,8.i-1} \quad (6)$$

The heat flow emitted by the oil in the section between $\vartheta_{F,8.i-1}$ and $\vartheta_{F,8.i+1}$ leads to an even increase in the PCM temperature. Within this section, the PCM temperature is determined by the measurement point $\vartheta_{PCM,8.i}$. In this case, the temperature at $\vartheta_{PCM,8.i}$ is used to determine the temperature of the wall in the section between $\vartheta_{F,8.i-1}$ and $\vartheta_{F,8.i+1}$.

For measuring the temperature of the PCM, the thermocouples (type K, accuracy class 2) have a deviation of +/- 0.44 K at a temperature of 59 °C. At an oil temperature of approximately 75 °C (corresponding to 612 counts), the deviation of the optical temperature measurement is +/- 0.80 K (7.1 counts). To reduce measurement error, the thermocouples and the optical measurement system are calibrated with the same reference thermocouple.

This calibration also includes the measurement uncertainty of the data acquisition and signal converter in the system. Therefore, all sensors show the same absolute temperature.

A statistical measurement uncertainty, however, still exists. In particular, inaccurate positioning of the glass fiber in the channel should be regarded as a source of error. In this case, the measurement error is +/- 0.23 K.

Results and discussion

Figure 8 shows the experimental set up of the storage tank while melting the PCM. This figure also provides an overview of the different types of heat transfer phenomena that occur while the PCM is melting.

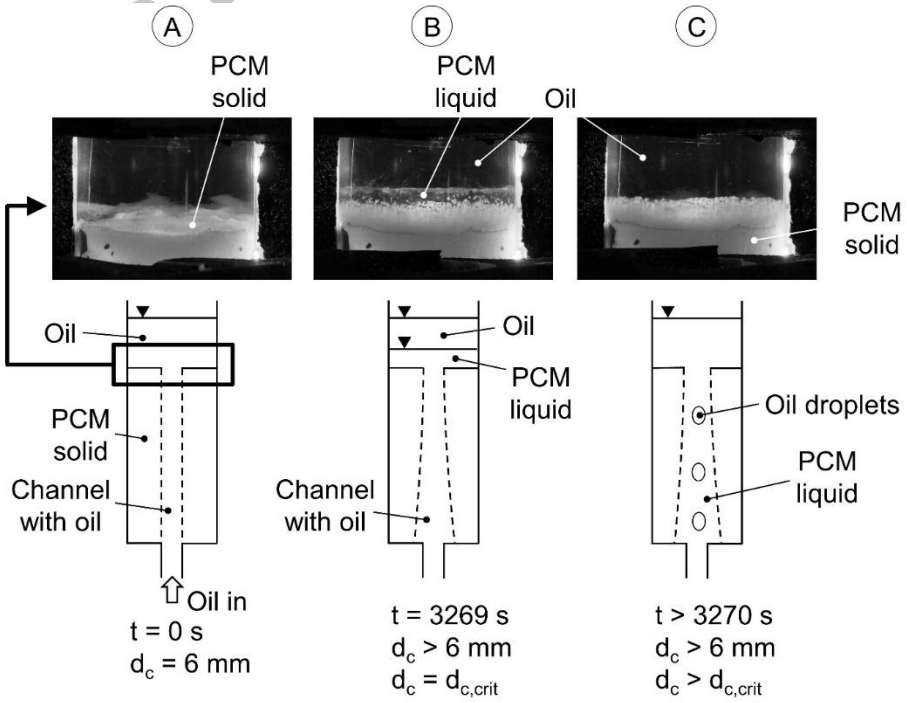

Figure 8: Illustration of the storage tank while melting the PCM with various types of heat transfer phenomena

ACCEPTED MANUSCRIPT

At t = 0 s, the channel diameter is 6 mm (Figure 8 A). The channel is completely filled with oil. During melting of the PCM, the inlet oil temperature is greater than the melting point of the PCM. As a result, the PCM in the channel is melting and the diameter of the channel increases. Part of the liquid PCM rises up with the oil mass flow and accumulates on top of the solid PCM. A part of the liquid PCM forms a liquid PCM layer at the solid wall. At 3269 s, a critical channel diameter is reached (Figure 8 B). After this point (Figure 8 C), the liquid PCM begins to fall down into the channel, and the channel becomes filled with liquid PCM. At this time, a different type of heat transfer occurs. Oil droplets rise up through the liquid PCM.

To illustrate the temporal dependence of these phenomena, the temperature at measurement point 8.1 is considered (Figure 9). At (Figure 9 A), the PCM around point 8.1 is solid, and the temperature increases. At (Figure 9 B), the PCM melts and is entrained with the oil flow to the top of the channel. On the way, the temperature of the liquid PCM decreases. At (Figure 9 C), the thermocouple at 8.1 is surrounded by oil and liquid PCM. After 3270 s (54.5 min), the liquid PCM is falling down into the channel, and the temperature at 8.1 drops suddenly (Figure 9 D). The channel is now filled with liquid PCM.

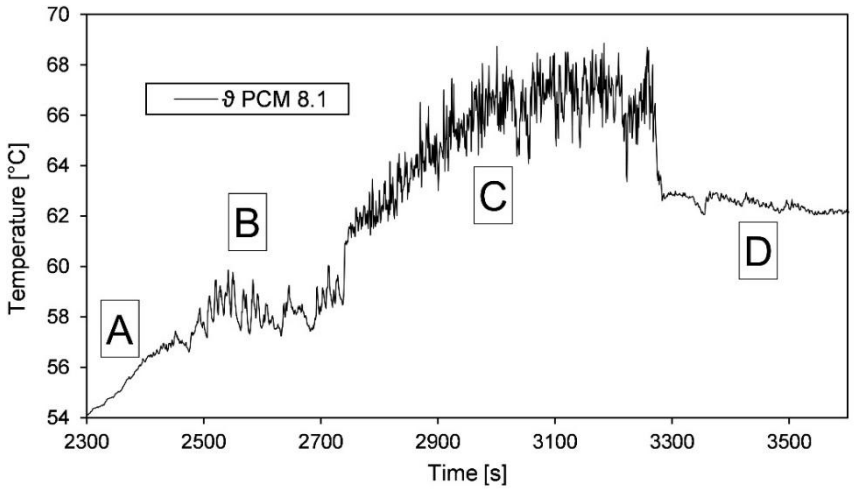

Figure 9: PCM temperature at measuring point 8.1 during melting of the PCM

Figure 10 shows the heat transfer coefficient obtained during melting of the PCM at an oil mass flow of 6.50×10^{-4} kg/s. The results illustrate how melting influences the heat transfer coefficient. The inlet temperature of the oil is 75 °C.

ACCEPTED MANUSCRIPT

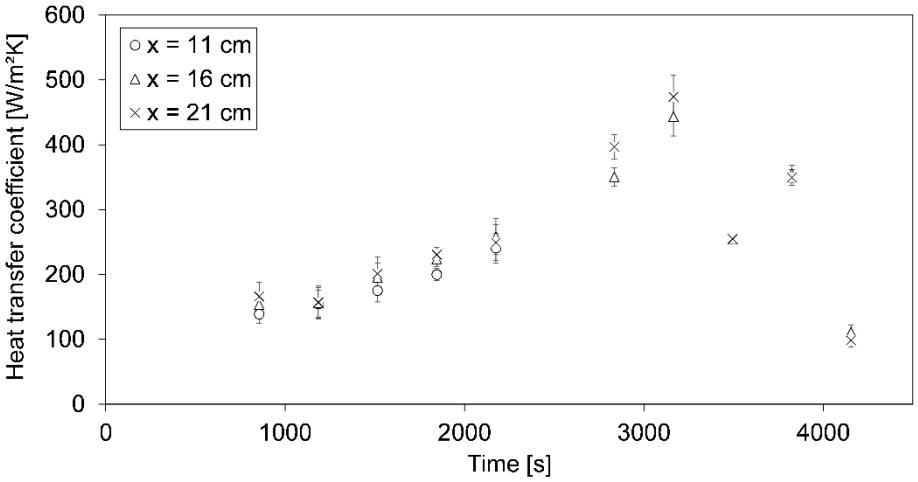

Figure 10: Heat transfer coefficient at an oil mass flow of 6.50 × 10^{-4} kg/s during melting of the PCM. The inlet temperature of the oil is 75 °C

It is obvious that the heat transfer coefficient increases with time corresponding to the proportion of liquid PCM. This is because the liquid PCM at the wall of the channel leads to a higher heat transfer as a result of increased turbulence between the oil and liquid PCM.

The maximum heat transfer coefficient of approximately 500 W/m²·K is reached at t = 3165 s. After this point, the heat transfer coefficient decreases. The channel becomes filled with liquid PCM, and the introduction of oil now leads to formation of droplets within the channel. From this point, the heat transfer phenomenon is changed.

Figure 11 shows the heat transfer coefficient between solid PCM and oil at three different oil mass flows (4.03 × 10^{-4}, 7.11 × 10^{-4}, and 11.5 × 10^{-4} kg/s). In this case, the inlet temperature is 56 °C. As the PCM does not melt, the geometry of the channel does not change. Each measurement value of the heat transfer coefficient is the mean value for the whole test section.

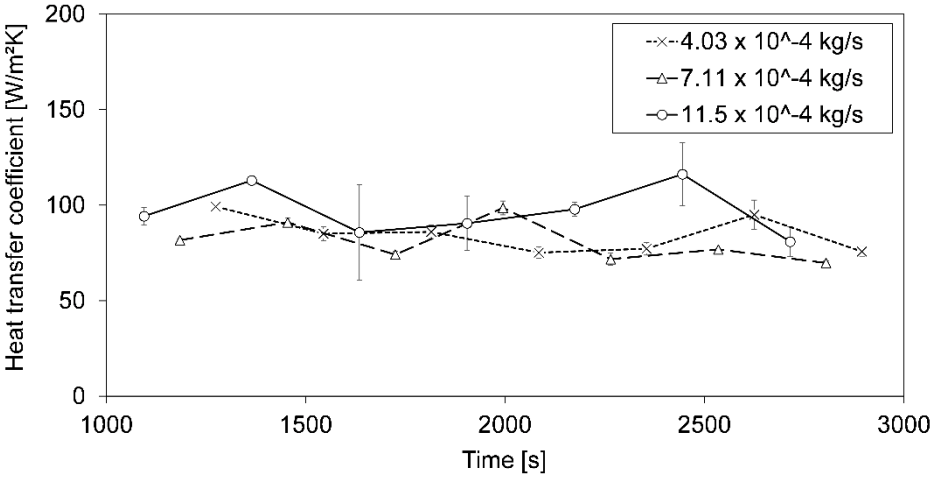

Figure 11: Mean heat transfer coefficients between solid PCM and oil at three different oil mass flows. The inlet temperature of the oil is 56 °C

These measurement results show that the mean heat transfer coefficient for the whole time period for an oil mass flow of 4.03 × 10^{-4} kg/s is 85 W/m²·K (+/- 9.8 W/m²·K). For an oil mass

ACCEPTED MANUSCRIPT

flow of 7.11 × 10^{-4} kg/s, the heat transfer coefficient is 80 W/m²·K (+/- 9.7 W/m²·K), while for an oil mass flow of 11.5 × 10^{-4} kg/s, the heat transfer coefficient is 97 W/m²K (+/- 12.3 W/m²·K). For a given channel flow, the heat transfer coefficient can be calculated theoretically according to equation (7):

$$\alpha = \frac{Nu \cdot \lambda_{HTF}}{L} \tag{7}$$

The Nußelt number can be calculated according to equation (8) [17]:

$$Nu = Nu_0 \cdot K_T \tag{8}$$

In this case the Nußelt number Nu is calculated from a base value Nu_0 and K_T. K_T can be calculated according to equation (9):

$$K_T = \left(\frac{Pr_m}{Pr_W}\right)^{0,11} \tag{9}$$

K_T takes the temperature dependence of the material values into account. Pr_W is the Prandtl number of the oil at wall temperature and Pr_m can be calculated according to equation (10):

$$Pr_m = \left(\frac{\Pr(\vartheta_{oil,in}) + \Pr(\vartheta_{oil,out})}{2}\right) \tag{10}$$

The base value Nu_0 can be calculated according to equation (11):

$$Nu_0 = \left[49{,}371 + \left(1{,}615 \cdot Gz^{1/3} - 0{,}7\right)^3\right]^{1/3} \quad \vartheta_W = const. \tag{11}$$

The theoretical heat transfer coefficient for an oil mass flow of 4.03 × 10^{-4} kg/s is 101 W/m²·K. For an oil mass flow of 7.11 × 10^{-4} kg/s, the theoretical heat transfer coefficient is 116 W/m²·K, while for an oil mass flow of 11.5 × 10^{-4} kg/s, the theoretical heat transfer coefficient is 135 W/m² K. Figure 12 shows the comparison of measured and theoretical heat transfer coefficients.

ACCEPTED MANUSCRIPT

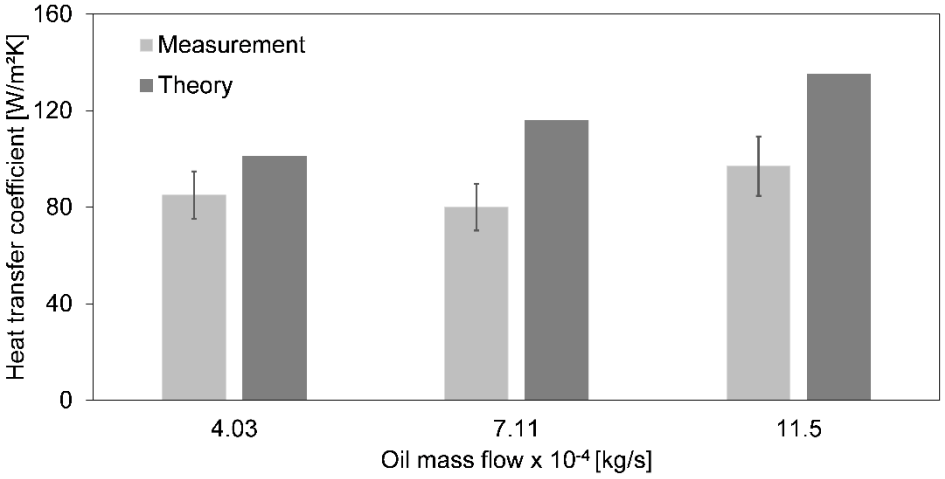

Figure 12: Comparison of measured and theoretical heat transfer coefficients

As can be seen the theoretical and measured heat transfer coefficients are similar in magnitude. The differences between the theoretical and measured values of the heat transfer coefficients can be caused by different effects like pipe roughness and will be investigated in future work.

These measurement results provide a deeper understanding of the heat transfer in a direct contact latent heat storage. In a first approximation, the determined heat transfer coefficients can be used to design real direct contact latent heat storage systems. There are indications that similar flow patterns exist in same parts of the real and artificial cylindrical channels. One indication is the ejection of liquid PCM out of the channel during melting of the PCM. This happened for the same oil mass flow for the real and artificial cylindrical channel. It can be a sign that there is an approximately equal flow velocity in both channels.

Conclusion

In this study, the heat transfer coefficient of solid and melted PCM was experimentally investigated in a direct contact latent heat storage consisting of a vertical cylindrical storage tank with a salt hydrate as the PCM and a mineral oil as the HTF. The results show the effect of the flow rate on the heat transfer coefficient (for solid PCM). Furthermore, the study shows the effect of an additional liquid PCM phase on the heat transfer coefficient by melting the PCM. From these observations, different types of heat transfer phenomena can be explained. The conclusions are summarized as follows:

1. When melting the PCM, the diameter of the channel increases. Liquid PCM partially accumulates on top of the solid PCM. Another part of the PCM forms a liquid PCM layer at the solid PCM wall. The channel diameter increases until a critical diameter is reached, at which point the liquid PCM falls down into the channel, and the channel becomes filled with liquid PCM. At this time, a different type of heat transfer occurs. Oil droplets rise up through the liquid PCM.
2. While melting the PCM, the heat transfer coefficient increases with the time respective to the proportion of liquid PCM until the point at which liquid PCM falls down into the channel.

ACCEPTED MANUSCRIPT

3. The heat transfer coefficient of solid PCM is nearly constant at approximately 87 W/m²K for all oil mass flows.

The determined heat transfer coefficients can be used for the design of direct contact latent heat storages and provide a deeper understanding of the heat transfer phenomena in a direct contact latent heat storage. The heat transfer coefficients can also be used for the scaling of these storage types.

ACCEPTED MANUSCRIPT

ACCEPTED MANUSCRIPT

References

[1] D. Aydin, S. P. Casey, S. Riffat, The latest advancements on thermochemical heat storage systems, Renewable and Sustainable Energy Reviews 41 (2015) 356-367

[2] P. Pardo, A. Deydier, Z. Anxionnaz-Minvielle, S. Rouge, M. Cabassud, P. Cognet, A review on high temperature thermochemical heat energy storage, Renewable and Sustainable Energy Reviews 32 (2014) 591-610

[3] T. Nomura, N. Okinaka, T. Akiyama, Technology of Latent Heat Storage for High Temperature Application: A Review, ISIJ International 50, No. 9 (2009) 1229-1239.

[4] H. Mehling, L. F. Cabeza: Heat and cold storage with PCM, Springer, Berlin Heidelberg, 2008, pp. 158-162

[5] F. Lindner, K. Scheunemann, Latent heat accumulator, Patent: US 4371029 A, 1983.

[6] F. Lindner, P. Tattermusch, Latentwärmespeicher: EP 0789214 A2, 1997.

[7] A. Kaizawa, H. Kamano, A. Kawai, T. Jozuka, T. Senda, N. Maruoka, T. Akiyam, Thermal and flow behaviors in heat transportation container using phase chage Materials, Energy Conversion and Management 49 (2008) 698-706.

[8] T. Nomura, M. Tsubota, T. Oya, N. Okinaka, T. Akiyama, Heat storage in direct-contact heat exchanger with phase change material, Applied Thermal Engineering 50 (2013) 26-34.

[9] T. Nomura, M. Tsubota, A. Sagara, N. Okinaka, T. Akiyama, Performance analysis of heat storage of direct-contact heat exchanger with phase-change material, Applied Thermal Engineering 58 (2013) 108-113.

[10] T. Nomura, M. Tsubota, T. Oya, N. Okinaka, T. Akiyama, Heat release performance of direct-contact heat exchanger with erythritol as phase change material, Applied Thermal Engineering 61 (2013) 28-35

[11] V. Martin, B. He, F. Setterwall, Direct contact PCM-water cold storage, Applied Energy 87 (2010) 2652-2659.

[12] S. Kunkel, F. Kübel-Heising, P. Dornhöfer, I. Medina, J. Weis, R. Stabler, J.-U. Repke, M. Rädle, Direct contact latent heat storage for efficiency enhancement of heat pumps, Chemie Ingenieur Technik 90 (2018) 234-240.

[13] H.-J. Steinbächer, J. Tedy, S. Kunkel, M. Rädle, J.-U- Repke, A. Nguyen, T. Schumacher, G. Brösigke, Latentwärmespeicher, Patent: DE 10 2014 103 108 A1, 2015.

[14] B. Zalba, J. M. Marin, L. F. Cabeza, H. Mehling, Review on thermal energy storage with phase change: materials, heat transfer analysis and applications, Applied Thermal Engineering 23 (2003) 251-283.

[15] Fragoltherm GmbH + Co. KG, product information sheet, Fragoltherm Q-7

[16] VDI-Gesellschaft, Berechnungsmethoden für Wärmeleitung, konvektiven Wärmeübergang und Wärmestrahlung, VDI-Wärmeatlas 11 (2013) pp. 31.

[17] R. Marek, K. Nitsche, Praxis der Wärmeübertragung, Grundlagen – Anwendungen – Übungsaufgaben, Hanser, München, 2007, pp. 187-190

ACCEPTED MANUSCRIPT

ACCEPTED MANUSCRIPT

Figure Captions and tables

ACCEPTED MANUSCRIPT

ACCEPTED MANUSCRIPT

Highlights

1. Heat transfer coefficients in a direct contact latent heat storage system were measured
2. Efficient optical temperature measurement in a rising oil phase
3. During melting of phase change material the heat transfer coefficient increases
4. The heat transfer phenomenon during melting of phase change material is changing

ACCEPTED MANUSCRIPT